

Chemical abundance anticorrelations in globular cluster stars: The effect on cluster integrated spectra

P. Coelho¹

Núcleo de Astrofísica Teórica, Universidade Cruzeiro do Sul, R. Galvão Bueno 868, Liberdade, 01506-000, São Paulo, Brasil; paula.coelho@cruzeirodosul.edu.br

S. M. Percival², M. Salaris²

Astrophysics Research Institute, Liverpool John Moores University, 12 Quays House, Birkenhead, CH41 1LD, UK; smp,ms@astro.livjm.ac.uk

ABSTRACT

It is widely accepted that individual Galactic globular clusters harbor two coeval generations of stars, the first one born with the ‘standard’ α -enhanced metal mixture observed in field Halo objects, the second one characterized by an anticorrelated CN-ONa abundance pattern overimposed on the first generation, α -enhanced metal mixture. We have investigated with appropriate stellar population synthesis models how this second generation of stars affects the integrated spectrum of a typical metal rich Galactic globular cluster, like 47 Tuc, focusing our analysis on the widely used Lick-type indices. We find that the only indices appreciably affected by the abundance anticorrelations are Ca4227, G4300, CN₁, CN₂ and NaD. The age-sensitive Balmer line, Fe line and the [MgFe] indices widely used to determine age, Fe and total metallicity of extragalactic systems are largely insensitive to the second generation population. Enhanced He in second generation stars affects also the Balmer line indices of the integrated spectra, through the change of the turn off temperature and – in the assumption that the mass loss history of both stellar generations is the same – the horizontal branch morphology of the underlying isochrones.

Subject headings: galaxies: star clusters: general — globular clusters: general — stars: abundances

1. Introduction

A large body of spectroscopic data published in the last 10 years has conclusively established the existence of primordial surface chemical abundance variations of C, N, O, Na – and sometimes of Mg and Al – in individual Galactic globular clusters (GCs) of all metallicities, from very metal rich objects like NGC6441, to the most metal poor ones like M15 (see, e.g., Carretta et al. 2010). When considering luminosities below approximately the red giant branch (RGB) bump level, within a given GC the chemical abundance patterns appear to be roughly the same all along the RGB down to the turn-off (TO) region (see, i.e. Gratton et al. 2001; Cohen & Meléndez 2005), and show CN and ONa (and sometimes also MgAl) anticorre-

lations for about 2/3 of the stars, superimposed onto a standard (i.e. consistent with the distribution found in field halo stars) α -enhanced heavy-element distribution ($[\alpha/\text{Fe}] \sim 0.3\text{--}0.4$). The anticorrelations display a range of negative variations of C and O accompanied by increased N and Na abundances, whose extension varies from cluster to cluster (Carretta et al. 2005, 2009). The remaining 1/3 of cluster stars shows an homogeneous standard α -enhanced metal mixture. At luminosities brighter than the RGB bump, observations point to the efficiency of some deep mixing process that decreases the surface C and increases N in all cluster stars (Yong et al. 2003; Gratton et al. 2004; Sneden et al. 2004), similarly to the case of field Halo stars (Gratton et al. 2000),

whereas the ONa pattern is essentially unchanged compared to lower luminosities. This effect varies from cluster to cluster, with a cluster like M13 depleting C much more efficiently than others (Smith & Martell 2003; Sneden et al. 2004).

The accepted working scenario to explain these CNONa anticorrelations prescribes that the stars currently evolving in a GC were born with the observed CNONa patterns. Intermediate-mass asymptotic giant branch (AGB) stars in the range $\sim 3 - 8M_{\odot}$ (and/or the slightly more massive super-AGB stars) and massive rotating stars are considered viable sources of the necessary heavy-element pollution (see, e.g., Ventura & D’Antona 2005; Decressin et al. 2007). Slow winds from the envelopes of AGB (or super-AGB stars) or from the equatorial disk formed around fast rotating massive stars inject matter into the intra-GC medium after a time of order $10^6 - 10^8$ yr, depending on the polluter. Provided that a significant fraction of the material is not lost from the cluster, new stars (second generation, but essentially coeval with the polluters’ progenitors, given their short evolutionary timescales) may be able to form directly out of pristine gas polluted to varying degrees by these ejecta, that will show the observed anticorrelation patterns. Another byproduct of this pollution may possibly be an enhanced initial He-abundance for these second generation stars. Recent numerical models by D’Ercole et al. (2008, 2010) have started to explore in quantitative details this broad picture.

If Galactic GCs are the local counterpart of extragalactic globulars, one should expect similar abundance anticorrelations to be imprinted in the integrated spectra of GCs populating the haloes of external galaxies. Given that GCs are employed as tracers of the star formation histories of spheroids (see, e.g. the review by Brodie & Strader 2006), and their spectra are usually modelled considering a simple stellar population (SSP) with a single initial chemical composition (and age), it is important to assess to what extent these abundance anticorrelations modify our interpretation of GC integrated spectra when compared to the case of a SSP. Also, integrated spectra of Galactic GCs are often used to test SSP models (see, i.e., Lee & Worthey 2005; Percival et al. 2009; Walcher et al. 2009; Vazdekis et al. 2010; Thomas et al. 2011) and the interpretation of these comparisons is clearly

dependent on the effect of these abundance anticorrelations on the cluster spectra.

We address for the first time these questions, focusing mainly on the predicted Lick-type absorption feature indices, that are routinely employed to determine ages and chemical compositions of extragalactic stellar populations (see, e.g., Burstein et al. 1984; Worthey 1994; Trager et al. 1998; Proctor et al. 2004; Puzia et al. 2005; Thomas et al. 2005; Graves & Schiavon 2008, and references therein). The next section presents our methodology and theoretical modelling, and is followed by an analysis of the results and a discussion.

2. Models

We have started our analysis by considering two α -enhanced SSPs – metal mixture with $[\alpha/\text{Fe}] \sim 0.4$ – with ages $t=12$ and 14 Gyr, $[\text{Fe}/\text{H}]=-0.7$ ($Z=0.008$) and initial He mass fraction $Y=0.256$, as representative of the first generation chemical composition in typical metal rich Galactic GCs, like 47 Tuc, whose integrated spectrum is often used for testing stellar population synthesis models. For both ages we have then considered a second generation population whose metal composition has C decreased by 0.30 dex, N increased by 1.20 dex, O decreased by 0.45 dex and Na increased by 0.60 dex with respect to the first generation α -enhanced mixture, all other metal abundances being unchanged. This pattern is typical of values close to the upper end of the observed anticorrelation patterns in Galactic GCs (Carretta et al. 2005, 2009). The metal distribution of this second generation coeval population has the same C+N+O sum and the same Fe abundance (as a consequence also the total metallicity Z will be practically the same) as the first generation composition, in agreement with spectroscopic measurements on second generation stars within individual Galactic GC¹.

For both the 12 and 14 Gyr second generation populations we have accounted for two alternative values of Y , e.g. $Y=0.256$ – as in the first stellar generation – and $Y=0.300$, to include a possi-

¹A well known exception to the constancy of Fe within a Galactic GC is ω Cen, that displays a large range of Fe abundances in addition to He enhancements and CNONa anticorrelations (see, e.g., Bellini et al. 2010, and reference therein).

ble enhancement of He in second generation stars. This latter choice is consistent with constraints on the typical enhancement of He in Galactic GCs, as determined by Bragaglia et al. (2010). We stress that these choices for the chemical composition of second generation populations are very general, and should give us a realistic estimate of their impact on GC analyses using SSPs. The accurate modelling of individual clusters would require, however, much more specific prescriptions, given that the distribution of CNONa abundances in second generation stars varies on a cluster-to-cluster basis. One would need to implement the effect of a continuous variations of CNONa elements up to the maximum values of the anticorrelations – that is cluster dependent – plus the exact number distribution of stars along the anticorrelation pattern, also cluster dependent. Even this would not help a detailed comparison with extragalactic GCs, given that at present we do not know – nor we can predict – the distribution of the abundance anomalies in these objects. The effect of the deep mixing along the upper RGB that modifies the CN abundances (that to some extent seems, again, cluster-dependent) is not accounted for in our calculations (nor in any other existing calculations of integrated spectra of GCs), but its effect goes in the same direction of the CN primordial anticorrelation, for it tends to amplify the range of C depletions and N enhancements.

Overall, our selection of representative extreme values of the CNONa variations will provide a first important indication of the maximum effect of these abundance anomalies on GC integrated spectra, and will serve as a guideline to interpret the abundance pattern derived from fitting SSPs to the observed spectra of Galactic and extragalactic GCs. We have considered in this first investigation on the subject one single $[\text{Fe}/\text{H}]$ value, typical of the metal rich subpopulations of Milky Way – and of 47Tuc, whose integrated spectrum is a benchmark for population synthesis models. The sensitivity of the spectra to the abundance anomalies may be quantitatively different when considering different $[\text{Fe}/\text{H}]$ values.

For each of the first generation SSPs we have then calculated synthetic integrated spectra as follows. The underlying isochrones are the BaSTI α -enhanced isochrones (with Reimers mass loss parameter $\eta=0.2$) by Pietrinferni et al. (2006),

with $[\text{Fe}/\text{H}]=-0.7$ ($Z=0.008$). The 12 and 14 Gyr isochrones representing the second generation populations are the same as the first generation α -enhanced ones with the appropriate Y abundance (taken from the BaSTI database), for we have verified with additional stellar model calculations that the effect of the two different metal mixtures on the isochrones is negligible, provided that the Fe abundance and the C+N+O sum are unchanged (see also Salaris et al. 2006).

We have then computed a grid of 57 stellar synthetic spectra for both first and second generation metal mixtures, that cover the gravity-effective temperature parameter space spanned by the corresponding 12 and 14 Gyr isochrones. The model atmospheres have been calculated using the code ATLAS12 (Kurucz & Avrett 1981; Kurucz 2005; Castelli 2005). Spectra were then computed with the code SYNTHE (Kurucz & Avrett 1981; Sbordone et al. 2004), for the wavelength region 3500 to 6000 Å and convolved to a spectral resolution $R = \lambda/\delta\lambda = 10000$. The atomic line list adopted in the computations is based on the compilations by Coelho et al. (2005) and Castelli & Hubrig (2004). Lines for the molecules C₂, CH, CN, CO, H₂, MgH, NH, OH, SiH and SiO from Kurucz (1993) were included for all stars, and TiO lines from Schwenke (1998) were included for stars cooler than 4500 K.

From the appropriate isochrone and grid of synthetic stellar spectra we have calculated the integrated spectrum for these first and second generation populations, employing the Kroupa (2001) initial mass function, and computed the corresponding values I of the standard Lick-type indices as defined in Table 2 of Trager et al. (1998), plus the H γ and H δ indices defined in Worthey & Ottaviani (1997). Of the 21 indices in Trager et al. (1998) we had to neglect TiO₁ and TiO₂, that are beyond the upper limit of the wavelength range of our spectra. The values of $I_{1st\ generation}$ and $I_{2nd\ generation}$ have been determined as in Percival et al. (2009), using the LECTOR program by A. Vazdekis² and measured directly on our high resolution spectra, i.e., they are not transformed onto the Lick system, for the community is rapidly moving to measure indices at higher resolution than the original Lick system, especially since the pub-

²available at <http://www.iac.es/galeria/vazdekis/index.html>

lication of models employing the MILES spectral library (Sanchez-Blazquez et al. 2006; Vazdekis et al. 2010). As a test, we have degraded the resolution of our spectra to 2.3 Å, the resolution of the MILES spectral library and repeated the analysis described below. Although the absolute values of the indices have a different zero point, the size of the differential effects due to varying metal mixtures (and He abundances) are unchanged.

To assess the impact of second generation stars on ages and chemical composition of unresolved GCs, we have chosen to compare our predictions with the values from the grid of α -enhanced SSPs by Percival et al. (2009), that spans a wide range of ages and metallicities. These spectra have been calculated employing the same BaSTI α -enhanced isochrones (with Reimers mass loss parameter $\eta=0.2$) used in this paper, the same Kroupa (2001) initial mass function, and the synthetic stellar spectral library by Munari et al. (2005). These SSP spectra we adopted as the source of a 'reference' grid of values I of the indices for first generation SSPs with $[\text{Fe}/\text{H}]$ between -1.84 and $+0.05$, and age t between 1.25 and 14 Gyr. We found small offsets in the reference index values for the 12 and 14 Gyr, $[\text{Fe}/\text{H}]=-0.7$, α -enhanced SSPs, when compared to our new ATLAS12 calculations, due to differences in the stellar spectral libraries. To ensure these small offsets do not play any significant role in our analysis, we have decided to use our new results in a purely differential way. For each of the selected ages and Y of second generation stars, we have determined from our calculations the differences $\Delta I = I_{2nd\ generation} - I_{1st\ generation}$. The differences ΔI have been then added to the corresponding index values for the 12 and 14 Gyr 'reference' (first generation) α -enhanced grid, to represent the corresponding coeval second generation. These are the index values employed in the analysis that follows.

3. Results and discussion

In the following we compare the values of I for the various indices in first and second generation populations with the same age, to quantify how Lick-type indices respond to the presence of a coeval second stellar generation with CNONa anticorrelations in individual GCs. It is important to

stress from the outset that all comparisons that follow give a quantitative estimate of the *maximum* effect on the Lick-type indices of GCs, for we are comparing a pure first generation with a pure second generation population with extreme values of the CNONa anticorrelations. In a real GC the distribution of CNONa abundances ranges (most probably because of the effect of dilution with pristine gas) from the values of the standard first generation α -enhanced mixture, to extreme values like the ones used in our modelling (and also, the specific properties of the CNONa distribution vary from cluster to cluster). One expects therefore that *in real GCs the variations ΔI will attain values somewhere within the range derived from our analysis.*

We have first analyzed the case of the same initial He-abundance in first and second generation stars. We have considered the 18 metal line indices that can be measured in our spectra, and assessed how significant are the corresponding differences ΔI , as follows. At a fixed age of 14 Gyr and for each index, we have estimated the metallicity $[\text{Fe}/\text{H}]'$ of the first generation population needed to match the I value of the second generation population. If $\Delta I=0$, first and second generation I values are the same, and the 'correct' metallicity $[\text{Fe}/\text{H}]'=-0.7$ of the first generation stars is required to enforce agreement. A value of ΔI different from zero requires instead a $[\text{Fe}/\text{H}]'$ different from -0.7 dex for the first generation stars, in order to match the indices of the second generation. Table 1 reports for each metal index the value of ΔI and the corresponding difference $\Delta[\text{Fe}/\text{H}]$ between $[\text{Fe}/\text{H}]'$ and the 'correct' first generation $[\text{Fe}/\text{H}]$. If we consider as significant $\Delta[\text{Fe}/\text{H}]$ differences above 0.1 dex, we find that the only metal indices appreciably affected by the abundance anticorrelations are Ca4227, G4300, CN₁, CN₂ and NaD. The first four indices are sensitive to the C, N, O abundances, while NaD is sensitive to the Na and C abundances (Trager et al. 1998; Korn et al. 2005; Prochaska et al. 2005; Schiavon 2007; Graves & Schiavon 2008). Not surprisingly, CN₁, CN₂ and NaD are the indices most affected. They display a large increase in the second generation population, and to calculate the corresponding $\Delta[\text{Fe}/\text{H}]$ we had to perform a linear extrapolation beyond the upper boundary of our available $[\text{Fe}/\text{H}]$ range. The values of the Ca4227 and

Table 1: Variations of the values of the Lick-type indices for our 14 Gyr old first and second generation populations, both with $Y=0.256$, and the corresponding $\Delta[\text{Fe}/\text{H}]$ differences (see text for details) .

Index	ΔI	$\Delta[\text{Fe}/\text{H}]$
H δ_{F}	-0.068	--
H γ_{F}	0.274	--
CN ₁	0.084	1.960
CN ₂	0.087	1.324
Ca4227	-0.651	-0.306
G4300	-0.572	-0.360
Fe4383	-0.073	-0.022
Ca4455	0.000	-0.000
Fe4531	-0.014	-0.006
C ₂ 4668	-0.115	-0.063
H β	-0.032	--
Fe5015	0.056	0.016
Mg ₁	0.000	0.000
Mg ₂	-0.004	-0.016
Mgb	-0.158	-0.039
Fe5270	0.004	0.002
Fe5335	0.010	0.005
Fe5406	-0.005	-0.004
Fe5709	-0.060	-0.068
Fe5782	0.012	0.022
NaD	1.346	0.733

NOTE.—Units are \AA but for the CN1, CN2 indices, whose values are expressed in magnitudes.

G4300 indices display an opposite behavior, decreasing in the second generation population. The other metal indices show much less significant variations, when judged on the basis of the associated $\Delta[\text{Fe}/\text{H}]$. All Fe and Mg indices are essentially unaffected, and the same is true for Ca4455, at odds with the behavior of Ca4227. The value of C₂4668 is also very weakly changed, possibly because the decrease of both C and O in the second generation population affect the index in opposite directions and the resulting net variation is very small (see, e.g. Trager et al. 1998).

We have then investigated the effect of the abundance anticorrelations on the Balmer line indices and cluster age estimates, by considering the $\text{H}\beta$ -Fe5406 and $\text{H}\beta$ -[MgFe] diagrams³ displayed in Fig. 1. These are two powerful diagrams to break the age-metallicity degeneracy and allow the estimate of, respectively, age and Fe-abundance, and age and total metallicity Z of SSPs (see, e.g., Worthey 1994; Thomas et al. 2005; Lee & Worthey 2005; Tantalò & Chiosi 2005; Percival et al. 2009, and references therein). Figure 1 confirms the robustness of these diagnostic diagrams. The position of the second generation populations on these diagrams is barely distinguishable from their coeval first generation counterparts. We have displayed in Fig. 1 also the $\text{H}\delta_{\text{F}}$ -Fe5406 and $\text{H}\gamma_{\text{F}}$ -Fe5406 diagrams, that essentially confirm the results obtained for the $\text{H}\beta$ index. The $\text{H}\gamma_{\text{F}}$ index is more affected by the chemical composition of the second generation population, and the value of the index increases, a behavior opposite to the case of $\text{H}\beta$ and $\text{H}\delta_{\text{F}}$. Ages from $\text{H}\gamma_{\text{F}}$ are younger by ~ 2 – 3 Gyr in second generation stars, but given that – as mentioned at the beginning of this section – in a real GC the variation ΔI of a generic index is expected to be somewhere within the range determined from our model spectra, the ‘real’ bias on the $\text{H}\gamma_{\text{F}}$ ages is probably smaller, at the level of ≈ 1 Gyr.

To summarize, the presence of a second generation of GC stars with unchanged He-content affects appreciably only the Ca4227, G4300, CN₁, CN₂ and NaD metal indices. Very importantly, the variation of Ca4227 goes in the direction to mimic a lower Ca abundance, if this index is used

³ $[\text{MgFe}] = \sqrt{\text{Mgb} \times \langle \text{Fe} \rangle}$, with $\langle \text{Fe} \rangle = (\text{Fe5270} - \text{Fe5335})/2$.

as a measure of the Ca content. Our results support Lee & Worthey (2005) suggestion that the effect of a second generation population with CNONa anticorrelations may explain the discrepancies they find when comparing Ca4227, CN₁, CN₂ and NaD index strength (on the Lick IDS system) from their α -enhanced SSP models, with data for Galactic and M31 GCs. On the other hand, age, Fe-abundance and Z inferred from $\text{H}\beta$ -Fe5406 and $\text{H}\beta$ -[MgFe] diagrams (or the $\text{H}\delta_{\text{F}}$ and, to a slightly smaller extent, the $\text{H}\gamma_{\text{F}}$ counterpart) are confirmed once again to be robust and insensitive to the chemical abundance pattern of second generation stars.

To close our analysis, we consider the case of the 14 Gyr second generation population with enhanced He-abundance ($Y=0.300$), also displayed in Fig. 1. The values of all metal indices in this second generation population are essentially identical to the $Y=0.256$ case, i.e. they are unaffected by the enhancement of He, but the Balmer line indices are changed by the increase of He. The values of $\text{H}\beta$, $\text{H}\delta_{\text{F}}$ and $\text{H}\gamma_{\text{F}}$ for this population are essentially identical to the 12 Gyr second generation population with $Y=0.256$. As a numerical test, we have determined from our new calculations all I values for the 14 Gyr second generation population isochrone with $Y=0.256$, but using the $Y=0.300$ spectra, and found that both metal and Balmer line indices are identical to the values obtained from the spectra with the appropriate $Y=0.256$. This means that the changes in $\text{H}\beta$, $\text{H}\delta_{\text{F}}$ and $\text{H}\gamma_{\text{F}}$ compared to the $Y=0.256$ case are due to differences in the underlying isochrone representative of the He-enhanced second generation population. The TO and main sequence of the underlying isochrone are hotter by ~ 100 K compared to the $Y=0.256$ isochrone. Given that the TO mass at fixed age is smaller (by about $0.07 M_{\odot}$ in our case) in the He-enhanced isochrone, and the total mass lost along the RGB is the same ($0.11 M_{\odot}$) because of our assumption of the same mass loss law in all populations, the mass evolving along the HB is smaller, hence the typical T_{eff} of HB stars is higher, again by ~ 100 K. These higher T_{eff} values for TO and HB increase the value of the Balmer line indices.

As a conclusion, the presence of a second generation of GC stars with enhanced He does not modify the results obtained for the metal lines for

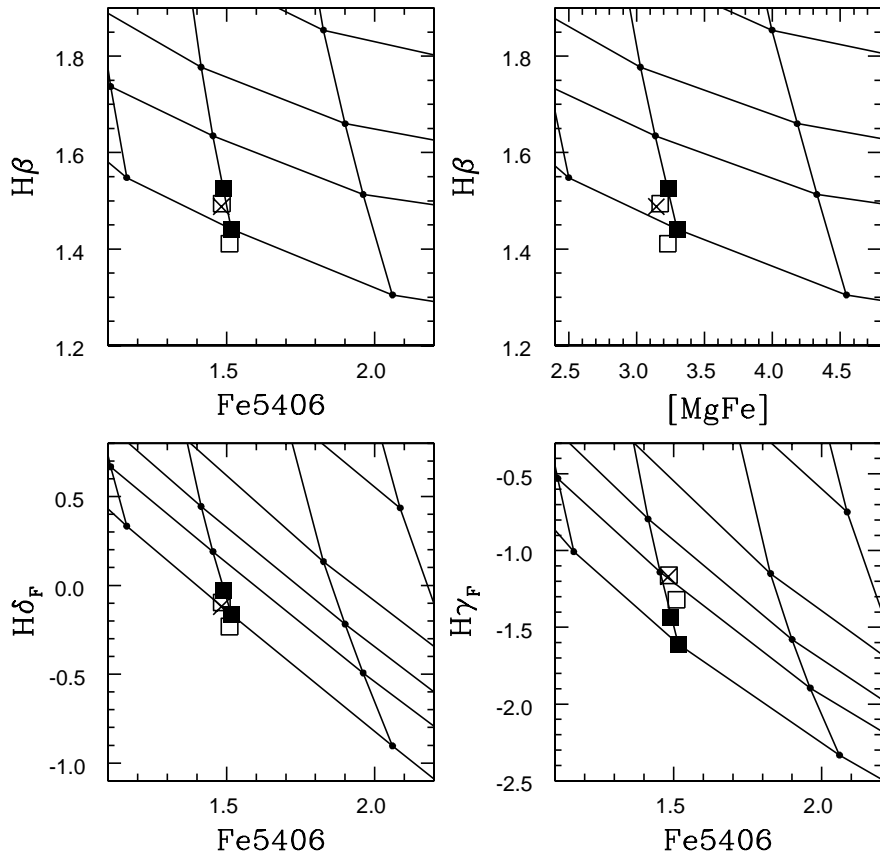


Fig. 1.— Several index-index grids for our reference α -enhanced SSPs. Metallicity increases from left to right (in the bottom two panels: $[Fe/H] = -1.01, -0.70, -0.29, +0.05$, corresponding to $Z = 0.004, 0.008, 0.01, 0.0198$), and age increases from top to bottom (in the bottom two panels: $t = 3, 6, 8, 10, 14$ Gyr). Filled squares denote the 12 and 14 Gyr first generation SSPs, open squares the corresponding second generation SSPs with $Y = 0.256$, whilst crosses denote a 14 Gyr second generation SSP with enhanced He (see text for details).

the case with $Y=0.256$, but impacts the Balmer line indices, through the T_{eff} change of TO and (assuming a similar amount of mass lost along the RGB in both first and second generation stars) HB stars. At low- and intermediate GC metallicities a small change in the HB evolving mass – induced for example by an enhanced He in second generation stars – is able produce very blue HB morphologies, that can have a huge impact on the cluster ages determined from Balmer line indices (see, e.g., De Propris 2000; de Freitas Pacheco & Barbuy 2000; Lee et al. 2000; Schiavon et al. 2004; Percival & Salaris 2011, and references therein).

Acknowledgements: PC acknowledges the financial support by FAPESP via project 2008/58406-4 and fellowship 2009/09465-0, and is grateful to Fiorella Castelli, Piercarlo Bonifacio and the KURUCZ-DISCUSS mailing list for the help with ATLAS and SYNTHÉ codes.

REFERENCES

- Bellini, A., Bedin, L. R., Piotto, G., Milone, A. P., Marino, A. F., & Villanova, S. 2010, *AJ*, 140, 631
- Bragaglia, A., Carretta, E., Gratton, R., D’Orazi, V., Cassisi, S., & Lucatello, S. 2010, *A&A*, 519, A60
- Brodie, J.P., & Strader, J. 2006, *ARA&A*, 44, 193
- Burstein, D., Faber, S. M., Gaskell, C. M., & Krumm, N. 1984, *ApJ*, 287, 586
- Carretta, E., Gratton, R. G., Lucatello, S., Bragaglia, A., & Bonifacio, P. 2005, *A&A*, 433, 597
- Carretta, E. et al. 2009, *A&A*, 505, 117
- Carretta, E., Bragaglia, A., Gratton, R. G., Recio-Blanco, A., Lucatello, S., D’Orazi, V., & Cassisi, S. 2010, *A&A*, 516, 55
- Castelli, F., & Hubrig, S. 2004, *A&A*, 425, 263
- Castelli, F. 2005, *Memorie della Societa Astronomica Italiana Supplement*, 8, 25
- Coelho, P., Barbuy, B., Meléndez, J., Schiavon, R. P., & Castilho, B. V. 2005, *A&A*, 443, 735
- Cohen, J. G., & Meléndez, J. 2005, *AJ*, 129, 303
- de Freitas Pacheco, J. A., & Barbuy, B. 2000, *A&A*, 302, 718
- D’Ercole, A., Vesperini, E., D’Antona, F., McMillan, S. L. W., & Recchi, S. 2008, *MNRAS*, 391, 825
- D’Ercole, A., D’Antona, F., Ventura, P., Vesperini, E., & McMillan, S. L. W. 2010, *MNRAS*, 407, 854
- Decressin, T., Meynet, G., Charbonnel, C., Prantzos, N., & Ekström, S. 2007, *A&A*, 464, 1029
- De Propris, R. 2000, *MNRAS*, 316, L9
- Gratton, R. G., Sneden, C., Carretta, E., & Bragaglia, A. 2000, *A&A*, 354, 169
- Gratton, R. G., Sneden, C., & Carretta, E. 2004, *ARA&A*, 42, 385
- Gratton, R. G., et al. 2001, *A&A*, 369, 87
- Graves, G. J., & Schiavon, R. P. 2008, *ApJ*, 177, 446
- Korn, A. J., Maraston, C., & Thomas, D. 2005, *A&A*, 438, 685
- Kroupa, P. 2001, *MNRAS*, 322, 231
- Kurucz, R. 1993, *Diatomic Molecular Data for Opacity Calculations*. Kurucz CD-ROM No. 15. Cambridge, Mass.: Smithsonian Astrophysical Observatory, 1993., 15,
- Kurucz, R. L. 2005, *Memorie della Societa Astronomica Italiana Supplement*, 8, 14
- Kurucz, R. L., & Avrett, E. H. 1981, *SAO Special Report*, 391,
- Lee, H., Yoon, S.-J., & Lee, Y.-W. 2000, *AJ*, 120, 998
- Lee, H.-c., & Worthey, G. 2005, *ApJS*, 160, 176
- Munari, U., Sordo, R., Castelli, F., & Zwitter, T. 2005, *A&A*, 442, 1127
- Percival, S. M., & Salaris, 2011, *MNRAS*, in press (arXiv:1012.0004)
- Percival, S. M., Salaris, M., Cassisi, S., & Pietrinferni, A. 2009, *ApJ*, 690, 427

- Pietrinferni, A., Cassisi, S., Salaris, M., & Castelli, F. 2006, *ApJ*, 642, 797
- Prochaska, L. C., Rose, J. A., & Schiavon, R. P. 2005, *AJ*, 130, 2666
- Proctor, R. N., Forbes, D. A., & Beasley, M. A. 2004, *MNRAS*, 355, 1327
- Puzia, T. H., Kissler-Patig, M., Thomas, D., Maraston, C., Saglia, R. P., Bender, R., Goudfrooij, P., & Hempel, M. 2005, *A&A*, 439, 997
- Renzini, A. 2008, *MNRAS*, 391, 543
- Salaris, M., Weiss, A., Ferguson, J. W., & Fusilier, D. J. 2006, *ApJ*, 645, 1131
- Sanchez-Blazquez P. et al., 2006, *MNRAS*, 371, 703
- Sbordone, L., Bonifacio, P., Castelli, F., & Kurucz, R. L. 2004, *Memorie della Societa Astronomica Italiana Supplement*, 5, 93
- Schiavon, R. P. 2007, *ApJS*, 171, 146
- Schiavon, R. P., Rose, J. A., Courteau, S., & MacArthur, L. A. 2004, *ApJ*, 608, 33
- Schwenke, D.W. 1998, *Chemistry and Physics of Molecules and Grains in Space – Faraday Discussions*, 109, 321
- Snedden, C., Kraft, R. P., Guhathakurta, P., Peterson, R. C., & Fulbright, J. P. 2004, *AJ*, 127, 2162
- Smith, G. H., & Martell, S. L. 2003, *PASP*, 115, 1211
- Tantalo, R., & Chiosi, C. 2004, *MNRAS*, 353, 917
- Thomas, D., Maraston, C., Bender, R., & Mendes de Oliveira, C. 2005, *ApJ*, 621, 673
- Thomas, D., Johansson, J., & Maraston, C. 2011, *MNRAS*, in press
- Trager, S. C., Worthey, G., Faber, S. M., Burstein, D., & Gonzalez, J. J. 1998, *ApJS*, 116, 1
- Ventura, P., & D’Antona, F. 2005, *ApJ*, 635, L149
- Vazdekis, A. et al. 2010, *MNRAS*, 404, 1639
- Walcher, J., Coelho, P., Gallazi, A., Charlot, S. 2009, *MNRAS*, 398, L44
- Worthey, G. 1994, *ApJS*, 95, 107
- Worthey, G., & Ottaviani, D. L. 1997, *ApJS*, 111, 377
- Yong, D., Grundahl, F., Lambert, D. L., Nissen, P. E., & Shetrone, M. D. 2003, *A&A*, 402, 985